Title

On Steady State Neutrino-heated Ultrarelativistic Winds from Compact Objects

Journal

The Astrophysical Journal, 561(2)

ISSN

0004-637X

Authors

Pruet, Jason
Fuller, George M
Cardall, Christian Y

Publication Date

2001-11-10

DOI

10.1086/322498

Peer reviewed

THE ASTROPHYSICAL JOURNAL, 561:957–963, 2001 November 10

ON STEADY STATE NEUTRINO-HEATED ULTRARELATIVISTIC WINDS FROM COMPACT OBJECTS

JASON PRUET,[1] GEORGE M. FULLER,[1] AND CHRISTIAN Y. CARDALL[2,3,4]
Received 2001 March 27; accepted 2001 June 12

ABSTRACT

We study steady state winds from compact objects in the regime where the wind velocity at infinity is ultrarelativistic. This may have relevance to some models of gamma-ray bursts (GRBs). Particular attention is paid to the case in which neutrinos provide the heating. Unless the neutrino luminosity is very large, $L > 10^{54}$ ergs s^{-1}, the only allowed steady state solutions are those where energy deposition is dominated by neutrino-antineutrino annihilation at the sonic point. In this case, the matter temperature near the neutron star surface is low, less than 1 MeV for typical neutrino luminosities. This is in contrast to the case for subrelativistic winds discussed in the context of supernovae, where the matter temperature near the neutron star approximates the temperature characterizing the neutrinos. We also investigate the setting of the neutron-to-proton ratio (N/P) in these winds and find that only for large (>10 MeV) electron-neutrino or electron-antineutrino temperatures is N/P entirely determined by neutrino capture. Otherwise, N/P retains an imprint of conditions in the neutron star.

Subject headings: gamma rays: bursts — neutrinos — relativity — stars: neutron

1. INTRODUCTION

We examine properties of ultrarelativistic winds from compact objects, and we thereby obtain insights into the special case where these winds arise from neutrino heating. Our principal motivation for the present study is to determine whether physically plausible steady state solutions exist in the ultrarelativistic regime and to determine the relation between neutrino parameters and the character of the outflow. A peculiar feature of the steady state ultrarelativistic solutions is that the matter temperature near the neutron star surface is cold. We comment below on whether or not this is physically realizable. We also study how the final neutron-to-proton ratio [or, alternatively, electron fraction, $Y_e = 1/(\mathrm{N/P} + 1)$], is set in these models. Only for large (>10 MeV) electron-neutrino or electron-antineutrino temperatures does Y_e in the initial wind material come into steady state equilibrium with the neutrino fluxes.

There is a rich literature concerning steady state outflow from neutron stars. In connection with supernovae, the neutrino-driven wind occurring several seconds post–core bounce is interesting because it is the favored candidate for the site of the *r*-process elements (Meyer et al. 1992; Woosley et al. 1994; Takahashi, Witti, & Janka 1994). The relation between neutrino parameters and the properties of the wind has been extensively discussed (Duncan, Shapiro, & Wassermann 1986; Qian et al. 1993; Qian & Woosley 1996). These studies were concerned with gentle, modest entropy winds, characterized by Lorentz factors of order unity far from the star.

Near the neutron star surface these gentle winds are well approximated as being in hydrostatic equilibrium. The temperature is set by the competition between neutrino-heating and neutrino-cooling terms, i.e., the matter temperature is roughly equal to the temperature characterizing the neutrinos. Apart from effects due to nucleosynthesis, the final electron fraction in these gentle winds is set by the ratio of electron-neutrino (ν_e) and electron-antineutrino ($\bar{\nu}_e$) capture rates on nucleons (Qian et al. 1993). The general relativistic extension of the wind equations, redshift factors, and neutrino trajectory bending has been discussed by Fuller & Qian (1996), Cardall & Fuller (1997), and Salmonson & Wilson (1999). These works also emphasize subrelativistic outflow velocities. Detailed studies of relativistic effects along these lines for *r*-process nucleosynthesis have been carried out recently by Otsuki et al. (2000).

In a pioneering study, Paczyński (1990) examined ultrarelativistic flow from neutron stars relevant for studies of gamma-ray bursts (GRBs). In this work no reference was made to a heating term, and except for photon diffusion, which is unimportant near the neutron star surface, the flow was assumed adiabatic. This work provided a detailed picture of the wind evolution far from the neutron star surface, which is the regime relevant for optical emission in GRBs. There are many similarities between these steady state ultrarelativistic winds and the fireballs discussed in connection with GRBs (Shemi & Piran 1990).

The present study is an attempt to fill the gap between detailed studies of the relation between neutrino heating and subrelativistic outflow and the study of ultrarelativistic outflow without reference to a heating mechanism. This is also a detailed look at the "guts" of a simple model for a GRB central engine. It may be applicable to the model proposed by Salmonson, Wilson, & Mathews (2001). In this model, binary neutron stars are compressed and heated as gravitational radiation saps orbital energy during the last seconds of inspiral. The heating drives copious neutrino loss ($L_\nu \sim 10^{52}$ ergs s^{-1}), which in turn drives a hot pair plasma from the neutron star surface.

Lastly, it has recently been argued that the electron fraction in neutrino-heated fireballs may be a clue to neutrino physics at the central engine, and may have observable consequences (Fuller, Pruet, & Abazajian 2000). The present study serves as a "proof of concept" of this idea for a simple

[1] Department of Physics, Code 0354, University of California, San Diego, 9500 Gilman Drive, La Jolla, CA 92093-0319.
[2] Physics Division, Oak Ridge National Laboratory, P.O. Box 2008, Oak Ridge, TN 37831-6354.
[3] Department of Physics and Astronomy, University of Tennessee, 401 Nielsen Physics Building, Knoxville, TN 37996-1200.
[4] Joint Institute for Heavy Ion Research, Oak Ridge National Laboratory, P.O. Box 2008, Oak Ridge, TN 37831-6374.

case. Interestingly, we find that the electron fraction in the wind far from the central engine is set by processes very near the central engine. If this is a generic feature of GRB central engine models, information about the electron fraction in GRBs may help pin down the central engine.

2. EQUATIONS

The general relativistic equations describing the outflow of material from the neutron star are Euler's equations:

$$\mathbf{u}\cdot(\nabla\mathbf{T}) = -\mathbf{u}\cdot(\nabla\mathbf{T}_\nu)\,,$$
$$(\mathbf{g}+\mathbf{u}\otimes\mathbf{u})\cdot(\nabla\mathbf{T}) = -(\mathbf{g}+\mathbf{u}\otimes\mathbf{u})\cdot(\nabla\mathbf{T}_\nu)\,, \quad (1)$$

baryon number conservation,

$$\nabla\cdot(\rho_b\,\mathbf{u}) \quad (2)$$

and the change in electron fraction due to lepton capture on baryons,

$$\mathbf{u}\cdot(\nabla Y_e) = (1-Y_e)(\lambda_{\nu_e n\to p}+\lambda_{e^+ n\to p}) - Y_e(\lambda_{\bar\nu_e p\to n}+\lambda_{e^- p\to n})\,. \quad (3)$$

In the above $\mathbf{u}$ is the 4-velocity of the outflowing material, $\mathbf{T}$ and $\mathbf{T}_\nu$ are the stress-energy tensors for the outflowing matter and the neutrinos, respectively, $\mathbf{g}$ is the metric tensor, and ρ_b is the rest mass energy density of baryons in the plasma comoving frame. In equation (3) $\lambda_{\nu_e n\to p}$ and $\lambda_{\bar\nu_e p\to n}$ are the capture rates for electron antineutrinos and electron neutrinos on neutrons and protons, respectively, and $\lambda_{e^+ n\to p}$ and $\lambda_{e^- p\to n}$ are the capture rates for positrons and electrons on neutrons and protons, respectively. In what follows we employ the Schwarzschild metric and use natural units, $G=c=\hbar=k_b=1$, with k_b the Boltzmann constant. In Schwarzschild coordinates the line element is

$$ds^2 = \mathbf{g}_{\mu\nu}\,dx^\mu\,dx^\nu = -(1-2M/r)^{-1}\,dr^2 + r^2\,d\Omega^2\,, \quad (4)$$

Here M is the mass of the neutron star and $d\Omega^2 = d\theta^2+\sin^2\theta\,d\phi^2$. Imposing steady state conditions and writing the radial component of the 4-velocity u^r as $u^r = vy$, where $y=(1-2M/r)^{1/2}/(1-v^2)^{1/2}$ and v is the outflow velocity of the plasma as measured in an inertial frame at rest in the Schwarzschild coordinate (t, r, θ, ϕ) system, allows us to rewrite the equations above as

$$(1-v^2)a\rho_b = (\rho+P)\left[\frac{vv'}{1-v^2}+\frac{M}{r^2}\frac{1}{(1-2M/r)}\right]+P'\,, \quad (5a)$$

$$q\rho_b = vy\left\{\rho'+(\rho+P)\left[\frac{v'}{v(1-v^2)}+\frac{M}{r^2}\frac{1}{(1-2M/r)}+\frac{2}{r}\right]\right\}, \quad (5b)$$

$$\dot M = 4\pi r^2\rho_b\,vy \quad (5c)$$

$$vyY_e' = (1-Y_e)(\lambda_{\nu_e\,\mathrm{n}\to\mathrm{p}}+\lambda_{e^+\mathrm{n}\to\mathrm{p}}) - Y_e(\lambda_{\bar\nu_e\,\mathrm{p}\to\mathrm{n}}+\lambda_{e^-\mathrm{p}\to\mathrm{n}})\,. \quad (5d)$$

In the above, primes denote differentiation with respect to r, and ρ and P are the total energy density (including rest mass) and pressure, respectively, of the plasma in the comoving plasma frame. $\dot M$ is the mass outflow rate. We have also introduced $a = -[(\mathbf{g}+\mathbf{u}\otimes\mathbf{u})\cdot(\nabla\mathbf{T}_\nu)]_r/\rho_b$ and $q = -\mathbf{u}\cdot(\nabla\mathbf{T}_\nu)/\rho_b$, which are, respectively, the momentum and energy deposition into the plasma per unit time per unit baryon rest mass. Phrasing our analysis in terms of quantities "per baryon" is convenient because the baryon number in a comoving volume is conserved. Also, we will see that whether or not the final flow is relativistic depends on how much heating and momentum deposition per baryon occurs.

The second law of thermodynamics and some algebra allows us to produce from these expressions two more first integrals of the flow:

$$\frac{ds}{dr} = \frac{m_b\,q}{Tvy}\,, \quad (6)$$

$$\frac{d(\hat H y)}{dr} = y[(1-v^2)a + q/(vy)]\,. \quad (7)$$

Here we have introduced the nucleon mass m_b, the entropy per baryon s (in units of Boltzmann's constant), and the enthalpy $\hat H = (\rho+P)/\rho_b$ of the plasma. It is useful to have explicit formulas for these quantities:

$$s = 5.21\rho_8^{-1}\left(\frac{T}{\mathrm{MeV}}\right)^3\,, \quad (8a)$$

$$\hat H - 1 \equiv H = \frac{Ts}{m_b}\,. \quad (8b)$$

In this equation ρ_8 is the density in units of 10^8 g cm^{-3}. The number 5.21 above becomes 1.89 as T decreases below the threshold for pair production. In writing equations (8a) and (8b) we have assumed that the electrons are nondegenerate and that the entropy of light particles dominates the entropy of nucleons (i.e., $s>20$). This is relevant for our analysis because we will be concerned principally with conditions near the sonic point, and we will show below that low entropy conditions near the sonic point cannot lead to ultrarelativistic flow at infinity. The quantity H is related to the quantity η, the ratio of energy density to rest mass energy density often discussed in connection with GRBs, through $\eta\sim(3/4)H+1$.

If the flow is to be relativistic at infinity, it must either be supersonic at the neutron star surface or pass through a sonic point somewhere above the neutron star. In the present work we focus on the case where the flow is not already supersonic at the neutron star surface. For the case of nondegenerate electrons and negligible baryon pressure ($s>20$), the equation governing v' can be written as

$$\frac{1}{v(1-v^2)}(1+H)(v^2-v_{\mathrm{sonic}}^2)v' = \frac{1}{r}\left[\frac{2}{3}H-(1+2H/3) \times (M/r)\frac{1}{1-2M/r}+ar(1-v^2)-\frac{qr}{3u^r}\right]. \quad (9)$$

From this equation we see that at the sonic point, the following conditions must be satisfied:

$$v^2 = v_{\mathrm{sonic}}^2 = \frac{H}{3}\frac{1}{H+1}\,, \quad (10a)$$

and

$$[1 - g(r)]\,\frac{2}{3}\,H = g(r) + \frac{qr}{3u^r} - (1 - v^2)ar\,. \qquad (10b)$$

In this last equation we have introduced

$$g(r) \equiv M/(r - 2M)\,, \qquad (11)$$

and $v^2_{\rm sonic} = (dp/d\rho)$ is the sound speed with the differentiation taken at constant entropy.

If for the moment we neglect the momentum deposition term, then equation (10b) implies that at the sonic point $qr/u^rH = 2(1 - g) - 3g/H \leq 2$. This is interesting because the change in entropy of the outflowing gas past the sonic point is implicitly given by

$$\int \frac{ds}{s} = \int \frac{qm_b}{Ts}\,\frac{dr}{u^r} = \int \frac{q dr}{u^r H} < \left(\frac{qr}{u^r H}\right)_{\rm sonic} \lesssim 1\,, \qquad (12)$$

Here the subscript "sonic" denotes values at the sonic point, and the second to last inequality holds if q/u^rH decreases more rapidly than r^{-1}. When the inequality in equation (12) holds, then, the entropy is approximately constant past the sonic point. Because the hydrodynamic equations imply that $3T'/T = s'/s - 2/r - u^{r\prime}/u^r$, the inequalities in equation (12) also imply that the temperature cannot increase substantially past the sonic point for accelerating flow. This implies that the enthalpy per baryon is roughly constant or decreasing past the sonic point. We then arrive at the important result that the final Lorentz factor of the wind is not much larger than the value of H at the sonic point when the above inequality is satisfied. For very large initial H, photon diffusion becomes important while the wind is still accelerating and the final Lorentz factor of the wind saturates at a correspondingly lower value (Grimsrud & Wasserman 1998; Shemi & Piran 1990). For typical wind luminosities $[(\dot{M}\hat{H}y)_\infty \sim 10^{51}$–$10^{52}$ ergs $s^{-1}]$ that we consider, photon diffusion is unimportant during the acceleration stage of the wind as long as $H < 10^4$–10^5. When the wind is roughly adiabatic during the acceleration stage, the final Lorentz factor of the wind occurs when the energy in relativistic particles $\sim H\rho_b$ has been converted to baryon kinetic energy (Paczyński 1990; Piran, Shemi, & Narayan 1993). The recognition that the final Lorentz factor of the wind is not much greater than the value of H at the sonic point will allow us to make important conclusions regarding the sonic point conditions needed in order that the final flow be relativistic.

In deriving equation (12) we neglected the momentum deposition term at the sonic point. Below we will show that this is a reasonable approximation for neutrino-driven winds. However, one could construct a heating term such that at the sonic point the heating and momentum deposition terms nearly cancel in equation (10b). In this case $qr/u^rH \gg 1$ at the sonic point is possible. In this case equation (7) implies that $(\hat{H}y)_\infty \lesssim (qr/v)_{\rm sonic}$, provided again that q/v drops sufficiently fast.

We can roughly divide the possible sonic point solutions into two families: those for which the terms involving the heating and momentum deposition terms q and a may be neglected (family I), and those for which these terms are important in determining the conditions at the sonic point (family II). As we will show, the neutrino energy deposition terms satisfy the inequalities in equation (12) when H and u^r increase with radius; therefore, only family II solutions can support steady state ultrarelativistic flow. An exception to this occurs when the sonic radius is very near $3M$. Previous discussions of steady state winds from neutron stars have focused on family I solutions. For these solutions $H \sim (3/2)M/(r - 3M)$ at the sonic point, and hence the sonic point must be near 3M in order to produce ultrarelativistic flow in the absence of heating terms (Paczyński 1990). For neutrino-driven wind studies relevant for the r-process, the heating terms are generally not important near the sonic point simply because those flows are subrelativistic or mildly relativistic, so that the sonic point occurs far from the neutron star where neutrino heating has fallen off.

For family II solutions (those where heating determines the sonic point conditions and drives the flow relativistically) some general observations can be made. If we assume that $H(r_s) \gg H(r_0)$ and $s(r_{\rm sonic}) \gg s(r_0)$ (where $r_{\rm sonic}$ is the Schwarzschild radial coordinate of the sonic point and r_0 is the initial radial coordinate of the flow, usually taken to be the neutron star radius here) then the sonic point condition and equation (7) imply

$$\int_{r_0}^{r_{\rm sonic}} \frac{yq}{u^r} \equiv y_{\rm eff} \int_{r_0}^{r_{\rm sonic}} \frac{q}{u^r} \sim \left[\frac{yqr}{2u^r(1 - g)}\right]_{\rm sonic}\,. \qquad (13)$$

In equation (13) we have defined $y_{\rm eff}$, we have assumed that $(1 - g)H \gg 1$ at the sonic point, and we have neglected the momentum deposition term a. Equation (13) serves to specify the position of the sonic radius given a heating term q and a velocity profile. If $q/u^r \propto r^{-\beta}$ (which occurs in steady state winds if the heating rate per unit volume drops as $r^{-\beta-2}$) the sonic point occurs at

$$\frac{r_{\rm sonic}}{r_0} \sim \left[\frac{2(\beta - 1)y_{\rm sonic}}{y_{\rm eff}(1 - g_{\rm sonic})} + 1\right]^{1/(\beta-1)}\,, \qquad (14)$$

which implies that the sonic point occurs near r_0 for rapidly dropping heating terms. Again the momentum deposition term a has been neglected in this approximation. Another interesting property of these winds is that the temperature does not vary greatly within the sonic radius if q is a decreasing function of radius. This is seen by noting that equations (6) and (13) imply

$$T_s^{-1} \sim \left(\frac{y_s}{y_{\rm eff}}\right) \frac{\int_{r_0}^{r_{\rm sonic}} q/Tu^r}{\int_{r_0}^{r_{\rm sonic}} q/u^r}\,, \qquad (15)$$

which allows us to define an effective temperature within the sonic point, $T_{\rm eff} = T_s\, y_s/y_{\rm eff}$.

The above equations allow us to extract the properties of ultrarelativistic steady state winds for arbitrary heating functions. We now turn to the particular case where neutrinos from the central compact object are responsible for the heating.

3. NEUTRINO-DRIVEN ULTRARELATIVISTIC WINDS

Perhaps the first question raised by a study of steady state neutrino-heated wind solutions is whether or not these winds are physically realizable for conventional compact objects. There are two parts to this question: (1) whether or not steady state can be achieved, and (2) whether or not the flow can be relativistic. We defer consideration of the second part until later, when we discuss mass ablation from the neutron star surface. While a hydrodynamic simulation is needed to determine the timescale to achieve steady state

in these winds, a rough estimate is that the equilibration timescale is of the order of the sound crossing time between the sonic radius and the neutron star surface, $\sim 10^{-4}$ s. This timescale is short compared with the neutrino diffusion timescale, which is of the order of seconds. The neutrino diffusion timescale governs the evolutionary timescale of the neutron star unless it undergoes a phase transition or becomes dynamically unstable. It is known that for most cold neutron star equations of state, general relativistic instability sets in for $r \sim 3M$. Below this radius the star becomes dynamically unstable and collapses on a dynamic timescale that is comparable to the equilibration timescale given above. For these small radius stars, then, it may not be sensible to put much stock in a steady state wind solution.

Before describing in some detail properties of the allowed steady state solutions, we must first examine the neutrino energy deposition terms. To parameterize the neutrinos we make the usual assumption that the neutrinos are emitted from a neutrinosphere with some radius r_0 (in this work we do not make a distinction between neutrinosphere radius and neutron star radius) and are characterized at the neutrinosphere by a Fermi-Dirac blackbody energy distribution with temperature T and zero chemical potential,

$$f_\nu = \frac{1}{e^{-E/T} + 1} \,. \tag{16}$$

This is a crude approximation to the actual expected energy spectra but suffices to mock-up the energy deposition physics (see Cardall & Fuller 1997). We further make the free streaming approximation, i.e., we neglect the fact that the neutrinos suffer a small depletion with increasing radius owing to interactions with the outflowing plasma. The facts that real neutron stars are characterized by some small but finite decoupling region over which the neutrino distribution function continues to evolve and that neutrinos from real neutron stars are, in general, nonthermal or better characterized by degenerate spectra are not important for our arguments. For a discussion of when it is appropriate to treat the neutrino as sharply decoupling from a neutrinosphere, see Salmonson & Wilson (1999).

Evaluating ∇T_ν for various neutrino plasma interactions is most easily accomplished by noting that Liouville's theorem implies that in an inertial frame at rest at some Schwarzschild coordinate r, the neutrino distribution function is characterized by the redshifted temperature

$$T_\nu(r) = T_\nu(r_0)\left(\frac{1 - 2M/r_0}{1 - 2M/r}\right)^{1/2} \equiv h T_\nu(r_0) \tag{17}$$

(see Fuller & Qian 1996), which also serves to define the redshift factor h, and a maximum angle of deviation from the radial direction given by

$$\cos\,\theta_{\max} \equiv x = \left[1 - \left(\frac{r_0}{r}\right)^2 \frac{1 - 2M/r}{1 - 2M/r_0}\right]^{1/2} . \tag{18}$$

The mass M of the neutron star appears in the expression for x because of the bending of null trajectories in the Schwarzschild geometry, as has been discussed by Cardall & Fuller (1997) and Salmonson & Wilson (1999).

In an inertial frame at rest in Schwarzschild coordinates, the contribution to $\nabla T_\nu \equiv (Q^{\hat{0}}_{\nu\bar{\nu}}, Q^{\hat{r}}_{\nu\bar{\nu}})$ from neutrino-antineutrino annihilation is

$$\begin{aligned} Q^{\hat{0}}_{\nu\bar{\nu}} &= \frac{G_F^2}{9(2\pi)^5}\, C T_\nu(r)^4 T_{\bar{\nu}}(r)^4 F_4(0) F_3(0) \\ &\quad \times [T_\nu(r) + T_{\bar{\nu}}(r)]\Phi(x) \,, \\ Q^{\hat{r}}_{\nu\bar{\nu}} &= \frac{G_F^2}{9(2\pi)^5}\, C T_\nu(r)^4 T_{\bar{\nu}}(r)^4 F_4(0) F_3(0) \\ &\quad \times [T_\nu(r) + T_{\bar{\nu}}(r)]\Psi(x)/4 \,. \end{aligned} \tag{19}$$

In the above, $\Phi(x) = (x-1)^4(x^2 + 4x + 5)$, $\Psi(x) = (x-1)^4(x+1)(3x^2 + 9x + 8)$, G_F is the Fermi constant, and hats are used to denote quantities in an inertial frame at rest in the Schwarzschild coordinate system. The quantities $F_3(0) = 7\pi^4/120$ and $F_4(0) \approx 23.3$ are the Fermi integrals of argument zero. The quantity C depends on the neutrino species. For $\nu_e\bar{\nu}_e$ annihilation $C = (1 + 2\sin^2\theta_W)^2 + 4\sin^4\theta_W$, where θ_W is the Weinberg angle ($\sin^2\theta_W \approx 0.23$), while for $\nu_\mu\bar{\nu}_\mu$ and $\nu_\tau\bar{\nu}_\tau$ annihilation $C = (1 - 2\sin^2\theta_W)^2 + 4\sin^4\theta_W$. For simplicity in what follows, we will assume that the luminosity of a single neutrino flavor gives all $\nu\bar{\nu}$ annihilation heating, and that for this flavor the neutrino and antineutrino temperatures are equal, $T_\nu = T_{\bar{\nu}}$. We will refer to this single neutrino flavor as μ or τ. This is merely a calculational device designed to reproduce the total heating rate from all neutrino flavors.

The contraction of the divergence of the neutrino stress-energy tensor with $\mathbf{u}$ and $\mathbf{g} + \mathbf{u}\otimes\mathbf{u}$ gives $\rho_b\, q_{\nu\bar{\nu}} = (1 - v^2)^{-1/2} Q^{\hat{0}}_{\nu\bar{\nu}}(1 - v\Psi/4\Phi)$ and $\rho_b\, a_{\nu\bar{\nu}} = (1 - v^2)^{-1}(1 - 2M/r)^{-1/2} Q^{\hat{0}}_{\nu\bar{\nu}}(\Psi/4\Phi - v)$. The terms entering the right hand side of the sonic point condition are then

$$\begin{aligned} \frac{r q_{\nu\bar{\nu}}}{3u^r} &= \frac{10^{-9} r_6}{(1 - v^2)^{1/2} u^r} \frac{[T_\nu(r)/\mathrm{MeV}]^9}{(T/\mathrm{MeV})^4}\, \Phi H\!\left(1 - \frac{v\Psi}{4\Phi}\right), \\ a_{\nu\bar{\nu}}(1 - v^2) r &= \frac{3 \times 10^{-8} r_6}{(1 - 2M/r)^{1/2}} \frac{[T_\nu(r)/\mathrm{MeV}]^9}{(T/\mathrm{MeV})^4}\, \Phi H\!\left(\frac{\Psi}{4\Phi} - v\right), \end{aligned} \tag{20}$$

where $r_6 = r/10^6$ cm. With these expressions we see that the neglect of the momentum deposition term within the sonic point is reasonable for winds driven by neutrino-antineutrino annihilation. At the sonic point the ratio of the energy and momentum deposition terms is typically greater than 2, so that there is not a near cancellation of the energy and momentum deposition terms.

Evaluation of the contribution to (∇T_ν) from neutrino-plasma interactions is complicated by the fact that an inertial observer comoving with the outflowing plasma sees a neutrino distribution function whose temperature varies with direction as $T_\nu(r)(1 - v\cos\theta)/(1 - v^2)^{1/2}$. The effect of this velocity- (and direction-) dependent redshift is to make the neutrino-plasma heating rates small as the outflow velocity becomes large. We will show that neutrino-antineutrino annihilation is the dominant heating term for the conditions of interest here. It suffices for us to note that in the limit where $v = 0$, the contributions to $(\nabla \mathbf{T}_\nu)$ from neutrino-electron scattering and neutrino capture on baryons are, respectively,

$$q_{\nu e} \sim 10\, q_{\nu\bar{\nu}} \frac{T^4}{T_\nu^4} \frac{1}{h^4} \frac{1 - x}{\Phi} \,, \tag{21}$$

if $T < T_\nu$, and

$$q_{\nu b} \sim 10^3 q_{\nu\bar{\nu}} \frac{T^4[T_{\bar{\nu}_e}^6 Y_e + T_{\nu_e}^6(1 - Y_e)]}{m_b h^3 H T_\nu^9} \frac{1 - x}{\Phi} . \quad (22)$$

Note that all of these heating terms satisfy the inequality in equation (12) if H increases with radius. Neutrino-antineutrino annihilation satisfies equation (12) because $q_{\nu\bar{\nu}}/H \sim \Phi r^2/(\dot{M}H)$, which falls more rapidly than r^{-6}. Neutrino electron scattering satisfies equation (12) because $q_{\nu e}/H \sim (1 - x) \sim r^{-2}$. Neutrino capture on baryons also satisfies this condition because $q_{\nu b}/H \sim (1 - x)/H$. These estimates for the scaling of the heating rates with radius neglect the dependence of the heating on the redshift factor h. This implies that the heating rates decrease even more rapidly with increasing radius if the wind is accelerating. This means that if the final flow is to be ultrarelativistic, we must have $H > 1$ at the sonic point, i.e., either $r_{\rm sonic} \sim 3M$,

$$T \sim 1 \text{ MeV} \left\{ \frac{r_6 \Phi(1 - g)[T_\nu(r)/10 \text{ MeV}]^9}{u^r} \right\}^{1/4} \quad (23a)$$

for $\nu\bar{\nu}$ annihilation dominating the heating,

$$T_\nu > 40 \text{ MeV } h^{-1} \left[\frac{1 - g}{r_6(1 - x)} \right]^{1/5} \quad (23b)$$

if electron-neutrino scattering dominates the heating rate, or

$$T_\nu > 30 \text{ MeV } h^{-1} \left[\frac{1 - g}{r_6(1 - x)} \right]^{1/6} \quad (23c)$$

if neutrino capture on baryons dominates. In equations (23a), (23b), and (23c) the values of all quantities are taken at the sonic point.

Unless the sonic radius occurs near $3M$ ($g \sim 1$), the neutrino temperatures needed to drive steady state ultrarelativistic flow imply extraordinary neutrino luminosities. (For example, consider the cases inherent in eqs. [23b] and [23c], $L \approx 10^{54} r_6^2 (T_\nu/20 \text{ MeV})^4$ ergs s^{-1}.) In what follows we therefore restrict ourselves to the case where $\nu\bar{\nu}$ annihilation dominates the heating at the sonic point and where only smaller, more realistic, neutrino luminosities are required.

3.1. *Steady State Flow when $\nu\bar{\nu}$ Annihilation Dominates at the Sonic Point*

Having determined that for modest neutrino luminosities ($L < 10^{54}$ ergs s^{-1}) ultrarelativistic steady state flow only occurs if $\nu\bar{\nu}$ annihilation heating dominates at the sonic point, we now turn to a discussion of the behavior of these solutions.

For $\nu\bar{\nu}$ annihilation the heating scales as $q/u^r \propto \Phi r^2 h^9 + O(v)$ and the sonic radius is readily estimated. This is shown in Figure 1. From this figure we see that the sonic radius is generically near r_0. Because $q_{\nu\bar{\nu}}/u^r$ decreases rapidly with radius, we may approximate $y_{\rm eff} \approx y(r_0)$ and $T_{\rm eff} \approx T(r_0) \approx (y_{\rm sonic}/y_{\rm eff}) T_{\rm sonic}$, which implies that the temperature is "cold" within the sonic radius so long as thermal neutrino energy losses are unimportant. Here "cold" means smaller than the neutrino energy distribution temperatures.

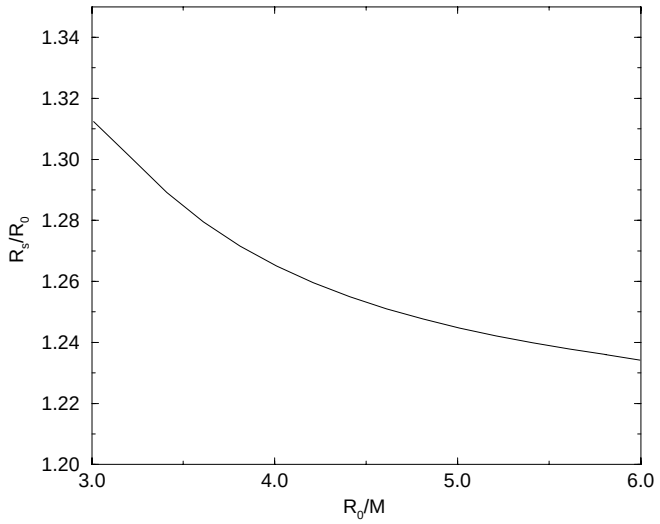

FIG. 1.—Approximate position of the sonic point as a function of r_0/M for neutrino-antineutrino annihilation dominating the heating term within the sonic radius. The momentum deposition term a has been neglected, and it is assumed that at the sonic point $H(1 - g) \gg 1$.

The mass ablation rate for $\nu\bar{\nu}$-dominated solutions is

$$\dot{M} \approx 10^{-4} (M_\odot \text{ s}^{-1}) \left\{ \frac{r_6^3 \Phi(1 - g)[T_\nu(r)/10 \text{ MeV}]^9}{H} \right\}_{\rm sonic} . \quad (24)$$

If $\dot{M}$ is too large the flow cannot be relativistic. This is the "baryon-loading problem" discussed in connection with GRBs. The relation between $\dot{M}$ and the neutrino-heating rates depends in detail on the structure of the compact object atmosphere below, above, and through the neutrinosphere. As argued by Fryer & Woosley (1998), obtaining a sufficiently low $\dot{M}$ may be particularly difficult for $\nu\bar{\nu}$ energy deposition because this heating rate drops so rapidly with radius. This requires that the density scale height above the neutrinosphere be small. For type II supernovae, calculations show that $\dot{M} \approx \dot{E}_\nu/(GM/r_0)$, where $\dot{E}_\nu$ is the integrated neutrino energy deposition rate (Woosley et al. 1994). This implies that most of the neutrino energy deposition goes into extracting baryons from the gravitational potential well of the neutron star. For supernovae, then, ultrarelativistic winds are not expected unless the early-time density scale height is smaller than expected or the late-time neutrino luminosities are larger than expected. Fryer & Woosley (1998) have argued that the baryon-loading problem cannot be overcome for mass ejection from strange stars resulting from the phase transition of a cooling or accreting neutron star, while Salmonson et al. (2001) have argued that neutrino heating during the compression of an inspiralling neutron star might lead to ultrarelativistic flow. The question must be considered for each proposed GRB site.

An estimate of $T_{\rm eff}$ allows a simple determination of the influence of neutrino capture on the electron fraction in the outflow. Noting that the number of neutrino captures per baryon n_c is approximately given by $dn_c = dr\, q_{\nu b}/(T_\nu u^r)$, where $\nu = \nu_e$ or $\bar{\nu}_e$ for neutrino capture on neutrons or protons, gives the total number of neutrino captures per

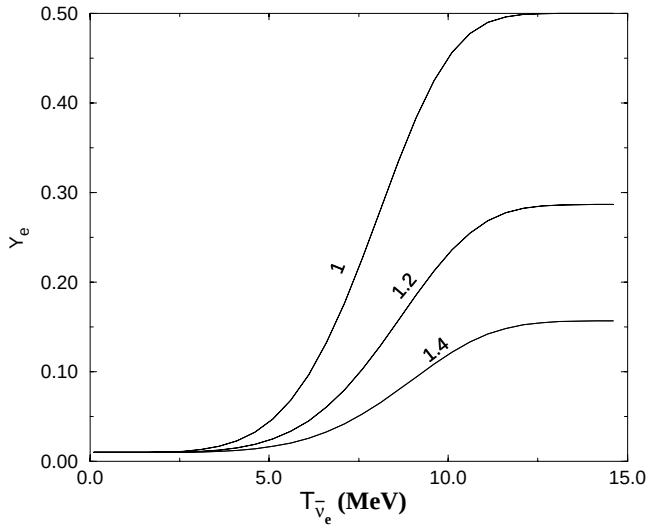

FIG. 2.—Final electron fraction in the fireball as a function of $T_{\bar{\nu}_e}$ and for different ratios $T_{\bar{\nu}_e}/T_{\nu_e}$ (labeled next to the curves). The initial electron fraction is taken to be 0.01, and the entropy of the plasma is assumed to increase by a factor of 10^5 as the plasma travels from the neutron star surface to the sonic point.

baryon between the neutron star surface and the sonic point

$$n_c \approx 10^{-6} r_6 [h^5(1-g)(1-x)]_{\rm sonic}(T_{\bar{\nu}_e}^5 + T_{\nu_e}^5)\ln(s_{\rm sonic}/s_0)\ , \tag{25}$$

where $s_{\rm sonic}$ and s_0 are the entropy at the sonic point and neutron star surface, respectively, and in this equation the neutrino temperatures are understood to be in MeV. With this expression we can solve for the final electron fraction in the fireball, neglecting e^+/e^- capture because of the low plasma temperature. Representative solutions are shown in Figure 2. This figure serves to illustrate the basic features of how the final electron fraction is set: (1) For low T_{ν_e} and $T_{\bar{\nu}_e}$, Y_e simply remains what it was in the neutron star. (2) As T_{ν_e} and $T_{\bar{\nu}_e}$ increase, the final Y_e tends toward equilibrium with respect to neutrino capture [i.e., $Y_e \rightarrow T_{\nu_e}^5/(T_{\nu_e}^5 + T_{\bar{\nu}_e}^5)$],

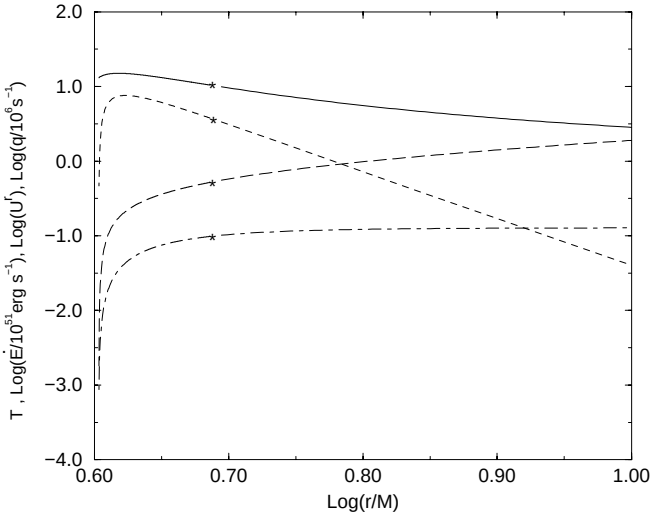

FIG. 3.—Evolution of a neutrino-heated wind solution as described in § 3.1. The solid curve is for temperature (in MeV), the short-dashed curve is for $q_{\nu\bar{\nu}}$, the long-dashed curve is for U^r, and the dot-dashed curve is for $\dot{E} = \dot{M}\hat{H}y$. The asterisks correspond to the position of the sonic point.

while still retaining some memory of the value of the electron fraction in the neutron star crust. Finally (3), for T_{ν_e} or $T_{\bar{\nu}_e} > 10$ MeV, Y_e is set ultimately by the competition between ν_e and $\bar{\nu}_e$ captures. If the neutrino temperatures are high and neutrinos set the electron fraction in the outflow, the final electron fraction is expected to be low because the neutrinos emitted from a neutron-rich star generically satisfy the temperature hierarchy $T_{\nu_e} \leq T_{\bar{\nu}_e}$. Because neutron star crusts typically have $Y_e < 0.1$, the electron fraction in the outflow is also expected to be low even when neutrino capture does not set the final electron fraction.

A numerical example of a steady state neutrino-heated wind leading to ultrarelativistic flow is shown in Figure 3. For this example we have taken $M = 1.4\ M_\odot$, $r_0 = 4M$, $T_{\nu_\mu} = T_{\bar{\nu}_\mu} = 10$ MeV, and $\eta = 3/4H + 1 \approx 100$ at the sonic point. The behavior of the wind near the neutron star is approximately independent of $H_{\rm sonic}$ as long as H is greater than a few. This is because in this limit ($H_{\rm sonic}$ is greater than a few), the pressure and energy density are dominated by relativistic light particles and not by baryons. Because of this, the temperature within the sonic point and the position of the sonic point are roughly independent of $H_{\rm sonic}$ (see eqs. [14] and [15]). This independence of the wind properties from $H_{\rm sonic}$ extends roughly until $r \sim (Hr)_{\rm sonic}$, where the thermal energy of the flow has been coverted to the kinetic energy of baryons and the wind begins to coast (Piran et al. 1993). Note, however, that the mass outflow rate scales as H^{-1} for given neutrino spectra.

The sonic radius can be chosen to match a particular entropy at the neutron star surface. Increasing $r_{\rm sonic}$ increases the entropy at the surface. The value of the surface entropy is very sensitive to changes in $r_{\rm sonic}$. Numerically, for $r_{\rm sonic}$ too large, the scale height for velocity changes becomes very small and the integration fails. Physically, the sonic radius is set by the requirement that the energy flow $\dot{E}$ at the sonic radius equals the net neutrino energy deposition rate interior to the sonic radius. Our plot only extends out to $r \approx 3r_0$. Past this radius neutrino energy deposition is unimportant and the flow satisfies the simple scaling laws given in Piran et al. (1993). The final Lorentz factor of the wind is approximately 150.

4. CONCLUSIONS

We have extended the study of steady state winds from compact objects to include the case where the wind is driven by a heating term and the wind velocity at infinity is ultrarelativistic. We find that for heating rates per unit volume that drop more rapidly than r^{-3}, the sonic point condition is dominated by the heating and momentum deposition terms, the sonic radius is near the compact object radius, and the temperature within the sonic radius is roughly constant.

Particular attention has been paid to the case where the wind is driven principally by neutrino energy deposition. For these winds neutrino-antineutrino annihilation dominates the heating unless the neutrino luminosity is very large ($\sim 10^{54}$ ergs s^{-1}). Interestingly, then, for a given neutrino luminosity there are an infinite family of steady state solutions. On one branch of this family is the usual subrelativistic solution discussed for supernovae, and on the other there exists a continuum of ultrarelativistic solutions dominated by neutrino heating at the sonic point. Of course, the low mass ablation rate needed for the ultrarelati-

vistic solutions may not be compatible with the structure of the atmosphere of the compact object near the neutrinosphere. This needs to be investigated for each compact object.

The way in which the electron fraction is set in the steady state winds we have discussed depends sensitively on the neutrino luminosity, with the number of neutrino captures per baryon varying as the fifth power of the neutrino temperature and depending only logarithmically on the final Lorentz factor of the outflow. For high ν_e or $\bar{\nu}_e$ temperatures the final electron fraction is set by neutrino capture. Otherwise, Y_e remembers its value in the neutron star crust. At least for a simple case, then, the electron fraction in the outflow is a diagnostic of conditions within the central engine. This is interesting because a priori one might guess that the electron fraction comes to equilibrium at $Y_e = 1/2$ or is always dominated by neutrino capture, as is the case for supernovae. It is also interesting because recently (Bahcall & Meszaros 2000) it has been argued that neutrinos arising from pion decay in GRB fireballs may be detectable. This neutrino signal depends, along with the other parameters characterizing the fireball, on the electron fraction in the fireball. If more realistic GRB central engine models also leave their fingerprints in the electron fraction in the outflow, such a signal might be used to distinguish between central engine models.

This work was partially supported by NSF Grant PHY 98-00980 at UCSD and an IGPP minigrant at UCSD. We are indebted to Jim Wilson and Jay Salmonson for useful insights.

REFERENCES

Bahcall, J. N., & Meszaros, P. 2000, Phys. Rev. Lett., 85, 1362
Cardall, C. Y., & Fuller, G. M. 1997, ApJ, 486, L111
Duncan, R. C., Shapiro, S. L., & Wasserman, I. 1986, ApJ, 309, 141
Fryer, C. D., & Woosley, S. E. 1998, ApJ, 501, 780
Fuller, G. M., Pruet, J., & Abazajian, K. 2000, Phys. Rev. Lett., 85, 2673
Fuller, G. M., & Qian, Y.-Z. 1996, Nucl. Phys. A, 606, 167
Grimsrud, O. M., & Wasserman, I. 1998, MNRAS, 300, 1158
Meyer, B. S., Mathews, G. J., Howard, W. M., Woosley, S. E., & Hoffman, R. D. 1992, ApJ, 399, 656
Otsuki, K., Tagoshi, H., Kajino, T., & Wanajo, S. 2000, ApJ, 533, 424
Paczyński, B. 1990, ApJ, 363, 218
Piran, T., Shemi, A., & Narayan, R. 1993, MNRAS, 263, 861
Qian, Y.-Z., Fuller, G. M., Mathews, G. J., Mayle, R. W., & Woosley, S. E. 1993, Phys. Rev. Lett., 71, 1965
Qian, Y.-Z., & Woosley, S. E. 1996, ApJ, 471, 331
Salmonson, J. D., & Wilson, J. R. 1999, ApJ, 517, 859
Salmonson, J. D., Wilson, J. R., & Mathews, G. J. 2001, ApJ, 553, 471
Shemi, A., & Piran, T. 1990, ApJ, 365, L55
Takahashi, K., Witti, J., & Janka, H. T. 1994, A&A, 286, 857
Woosley, S. E., Wilson, J. R., Mathews, G. J., Hoffman, R. D., & Meyer, B. S. 1994, ApJ, 433, 229